BIOSCIENCES BIOTECHNOLOGY RESEARCH ASIA, March 2025. Vol. **22**(1), p. 375-394

Development and Characterization of Luteolin Loaded Niosomesfor Effective Deliveryin Wound Healing

Devwati Puri[1], Harish Bhardwaj[1,2] and Rajendra Kumar Jangde[1]*

[1]Department of Pharmacy, University Institute of Pharmacy,
Pt. Ravishankar Shukla University, Raipur, Chhattisgarh, India.
[2]Department of Pharmacy, Shri Rawatpura Sarkar College of Pharmacy,
Shri Rawatpura Sarkar University Raipur, Chhattisgarh, India.

http://dx.doi.org/10.13005/bbra/3369

(Received: 03 December 2024; accepted: 07 March 2025)

This study focuses on the development of luteolin-loaded niosomes aimed at enhancing the therapeutic efficacy and bioavailability of luteolin for wound healing applications. Luteolin, despite its potential, faces significant limitations such as low absorption, poor water solubility, and reduced bioavailability. To overcome these challenges, a sustained-release formulation of luteolin-loaded niosomes was developed for topical application. The formulation was optimized using Design Expert software (Version 11) inBox-Behnken Design (BBD) through response surface methodology. Niosomes were prepared via the thinfilm hydration method, with three factors and two levels used in the optimization process. The niosomal preparationswere evaluated by polydispersity index (PDI), zeta potential, vesicle size, entrapment efficiency (EE), Fouriertransform infrared spectroscopy (FTIR), and in-vitro drug release profile. The optimized luteolin-loaded niosomes showed a vesicle size of 267.2 nm, a PDI of 0.34, a zeta potential of -20.25 mV, and an EE of 78.31%. In-vitro drug release studies established a sustained release of 67.08% over 12 hours. These results demonstrate that the developed luteolin-loaded niosomal formulations have the potential for sustained release, improving the therapeutic efficacy of luteolin in wound healing applications. This formulation shows promise in addressing the bioavailability issues of luteolin and enhancing its effectiveness in wound management.

Keywords: Luteolin; Niosome; Thin film-hydration method; Wound healing.

Wound healing represents a formidable dual challenge in the realms of therapy and finance within medicine.[1] Growth hormones, cytokines, antioxidants, the availability of metal ions (calcium, magnesium, and zinc), and growth hormones all play significant roles in the intricate process of wound healing. Wounds result from the integrity of the body's tissue. It can be triggered by physical, chemical, thermal, microbiological, or immunological damage, resulting in major clinical problems.[2] Chronic wounds may occur as a result of improper or interrupted healing. The whole body may suffer as a consequence of cutaneous damage that is either chronic (such as diabetes ulcer) or acute (such as surgery, mechanical injury, burns, etc.). As anoutcome, wound healing multistep is crucial for human health maintenance and comfort.[3,4] Wound healing is a complex biological process necessary for tissue restoration and recovery. This intricate journey involves four

*Corresponding author E-mail: rjandepy@gmail.com

sequential and overlapping steps: hemostasis, inflammation, proliferation, and remodeling, each playing a distinct role in achieving optimal healing outcomes.[5] Despite the well-defined stages, the effectiveness of wound healing can be influenced by multifaceted factors, including patient-specific variables, the wound's nature, and underlying health conditions. Recognizing and navigating these limitations is essential for tailoring therapeutic strategies and advancing our understanding of the intricacies involved in wound healing.[6,7]

Luteolin is a potential anti-inflammatory and antioxidant bioflavonoid polyphenolic phytoconstituent.[8] Additionally, reports of its potential antibacterial, immunomodulatory, gastroprotective, anti-tumour, cardioprotective, and anti-diabetic activities have also been made. A luteolin treatment led to faster wound healing, better epithelium regeneration, more collagen, stronger tensile strength, and reduced inflammation.[9,10] Luteolin exhibits several limitations, including low absorption, poor water solubility, and reduced bioavailability. Lutein metabolism and absorption have been studied in *vitro*using microsome and Caco-2 cellsobtained from the intestinal or liver of rats and humans. In accumulation, luteolin and luteolin-richplantswere the focus of pharmacokinetic research in humans and animals. However, few in vivo studies have been conducted on luteolin's distribution, absorption, metabolism, and bioavailability.However, it has a low bioavailability, which impacts its biological characteristics and effectiveness.[11,12] Many drug delivery techniques employing lipid carriers and nanoformulations have been developed to improve drug bioavailability.To increase bioavailability and efficacy, luteolin has been loaded into a variety of nanoformulations, including nanoparticles[13], NLCs[14], ROS-responsive nanoparticles modified by folic acid[15], and nanospheres.[16-18]

The application of luteolin vesicles in wound healing has not been documented in prior research. Lipid-based nanovesicles for topical distribution have increased the therapeutic effect throughout the past few decades. Transferosomes, ethosomes, niosomes, and cubosomes are a few examples of the several forms of nanovesicles that are employed for topical distribution. Cholesterol, surfactants, phospholipids, and water make up these vesicles. These carriers can encapsulate drugs that are both hydrophobic and hydrophilic. They can administer drugs to the bloodstream and skin.[19,20] Vesicles can shield medications from inadequate absorption into the skin blood vessels. It aids in maintaining the medicines at the skin's surface. Additionally, combining with the stratum corneum and changing the lamellae facilitates skin permeability through an intercellular lipid matrix. Drugs with low, medium, or high molecular weights can penetrate it.[21,22] Niosomes drug delivery system is the best technique to overcome luteolin's bioavailability and poor water solubility and improve its delivery. Cholesterol and non-ionic surfactant self-assemble to generate niosomes, which are bilayer-shaped non-ionic surfactant vesicles.Niosomes reduce the cost of wound management and enhance bioavailability by addressing the issue of insolubility.[23] The topical application of luteolin-loaded niosomes improves skin permeation.

This research aims to develop luteolin-loaded niosomes using the thin film hydration technique to improve wound healing. By encapsulating luteolin within niosomes, we aim to enhance drug bioavailability, minimize adverse effects, and establish sustained drug release. This approach offers a novel solution for expedited wound healing with reduced side effects compared to conventional methods. The thin film hydration technique is chosen for its ability to produce stable and uniform vesicles, ensuring optimal drug encapsulation and release. Overall, this study seeks to provide a rationale for the use of niosomes in wound care therapeutics.

MATERIALS AND METHODS

Materials

Luteolin was sourced from Prince Scientific (Hyderabad, India). Cholesterol, chloroform, and Span 60 were acquired from Loba Chemie Pvt. (Maharashtra, Mumbai, India). Methanol and PBS (Phosphate Buffered Saline pH 7.4) were obtained from Avantor Performance Material India Ltd. (Thane, India).

Methods

Experimental design

While designing a drug delivery system, independent variables affect the results of the

objective function. BoxBehnken Design (BBD) was utilised to formulation parameters optimize for manufacturing LUT-loaded niosomes. The optimization technique determines the link between dependent and independent variables. LUT-loaded niosomes were prepared by using cholesterol (X_1), surfactant (X_2), and sonication time (X_3) as independent variable at low (-1) and high (+1) levels. Vesicle size (R_1), EE (R_2), and DR (R_3) were taken as dependent variables (Table 1). Each composition had the same amount of LUT.

The experimental design gave 15runs with 3center points (all with identical conformation to check for errors), and their impacts on three dependent variables, such as vesicle size (R1), entrapment efficiency (R^2), and DR (R^3), were evaluated. The Design Expert software generated the polynomial quadratic equation, 3D response surface plots, and contour plots. The polynomial equation resulting from the factorial design is shown in Eq. no 1.

$$R = \beta_0 + \beta_1X_1 + \beta_2X_2 + \beta_3X_3 + \beta_4X_1X_2 + \beta_5X1X_3 + \beta_6X_2X_3 + \beta_7X_1^2 + \beta_8X_2^2 + \beta_9X_3^2 \quad ...(1)$$

Where, β_0, β_i(i = 1, 2, ……..9) and X_1, X_2, X_3 are the response R's intercept, linear coefficients, and the interaction term, in that order.

Percentage bias was considered by the following Eq. no 2.

$$\%Bias = [(Predicted\ value – Experimental\ value) / Predicted\ value] \times 100 \quad ...(2)$$

Preparation of LUT-loaded Niosomes

Niosomeswereformulated by thinfilm hydration technique. The LUT (50 mg), cholesterol (X_1), and surfactant (X_2), which were administered in the proportions specified as given in Table 2, were carefully weighed and dissolved in chloroform and methanol (10 mL, 1:1) in a round bottom flask. The organic solventwereevaporated at 40 ÚC and 100 rpm speed for 30 minutes using a rotary evaporation (IKA RV10 Digital Rotary Evaporator, IKA Pvt. Ltd., India), resulting in a thin film of surfactant formed on the flask wall. From the evaporator, the flask was removed and kept overnight in a desiccator under the vacuum to trace to organic solvent and removed. The dried thin film was rehydrated with PBD (pH 7.4) 10 mLat 55 ÚC for 30 min with gentle agitation. It forms a milky niosomal dispersion.

The niosomal suspension was then sonicated in a bath sonicator at different time points, as shown in Table 2, to reduce the vesicle size. The prepared niosomal suspensions were stabilized by keeping them at refrigerator temperature. According to the experimental design, all the formulations were prepared using a similar procedure.[24] The chosen ratios for components and sonication times in niosomes preparation are crucial for optimal vesicle formation, stability, and drug encapsulation. They are determined through empirical experimentation and optimization studies to achieve desired characteristics. Cholesterol, surfactant, and luteolin ratios are carefully balanced for stability and drug release kinetics, while sonication times are varied to achieve the desired vesicle size distribution for effective drug delivery. These parameters are selected based on a combination of literature review and experimental optimization to produce niosomes formulations suitable for their intended application.

Characterization of the prepared luteolin-loaded niosomes

Vesicle morphology

The samples were sputter-coated with gold for 3 minutes under a vacuum to assess the vesicles' nanostructure and surface morphology. Subsequently, they were examined using scanning electron microscopy (SEM Coxem EM-30, Korea).

Vesicle size, PDI, and Zeta potential

ZetaSizer (Malvern Zeta Sizer Pro, UK) was used to measure vesicle size, size distribution (PDI), and surface charge (ZP).The formulation (0.1 mL) was double distilled water diluted to supply an appropriate scattering intensity and scanned. PDI was examined to indicate the homogeneity of the vesicle size, and ZP was used to measure the surface charge. [25-27]

Entrapment Efficiency (EE) and Drug Loading

The centrifugation method measured the %EE and %DL of LUT-loaded niosomes (Eppendorf Centrifuge 5430 R, India, Ltd.). The 1.5 mL sample was centrifuged for 1 hour at 4°C at 10,000 rpm. A UV spectrophotometer (Shimadzu 1800, Japan) was used to find the free-drug concentration in supernatant liquid[28,29].following Eq., no 3. was used to calculate the %EE:

$$\%EE = [(C_t - C_f)/C_t] \times 100 \quad ...(3)$$

Where Ct represents drug concentration total, and Cf represents free-drug concentration. The %DL was calculated by the following Eq. no 4.

$$\%DL = [(C_t - C_f) / \text{Weight of the lipids}] \times 100 \quad ...(4)$$

Fourier transform infrared (FTIR)

FTIR spectrum analysis was conducted utilizing a Bruker FTIR instrument (Bruker FTIR Alpha 2, USA and USA and PerkinElmer L1600300 Spectrum TWO LiTa, Llantrisant, UK) was used to check the compatibility between LUT, span 60, cholesterol and LUT loaded Niosome used.They were retaining the potassium bromide (KBr) disc method. A background blank KBr pellet was used for analysis, and the baseline was adjusted accordingly. The samples were scanned within a wave number range from 400 cm{ ¹ to 4000 cm^{-1}, with a high-resolution set at 1.0 cm{ ¹. [30]

In-*vitro* Drug Release

The in *vitro* release of niosomes was determinedutilizing a dialysis bag.The niosomes that were prepared were placed separately in the dialysis bag, which served as a donor compartment. The dialysis bag was then dipped into a beaker of 250 mL PBS pH 7.4containing receptor compartment. The bag was kept at a constant

Table 1. Levels ofvariables utilised to optimize LUT-loaded niosomes using BBD

Factors	Units	Code	Levels	
			Low (-1)	High (+1)
Independent variables				
Cholesterol	mg	X_1	20	50
Span 60	mg	X_2	40	100
Sonication time	min	X_3	3	5
Dependent variables				
Vesicle size	nm	R_1		
EE	%	R_2		
DR	%	R_3		

Table 2. The study investigates distinct batches of LUT-loaded niosomes, delineating the independent variables, their specific levels, and the corresponding response values

Std	Run	Factors			Response		
		X_1(mg)	X_2(mg)	X_3(min)	R_1(nm)	R_2(%)	R_3(%)
1	1	20	40	4	331	63.86	85.02
15	2	35	70	4	257	80	64.52
4	3	50	100	4	451	69.35	74.92
7	4	20	70	5	392	65.24	75.52
6	5	50	70	3	419	69.44	84.75
5	6	20	70	3	286	64.38	87.32
14	7	35	70	4	262	81.12	63.2
11	8	35	40	5	244	77.2	79.47
8	9	50	70	5	251	68.39	77.11
3	10	20	100	4	310	74.35	73.02
10	11	35	100	3	342	72.58	80.9
12	12	35	100	5	422	79	67.75
9	13	35	40	3	374	75.33	71.4
2	14	50	40	4	238	86	78.62
13	15	35	70	4	266	81.12	62.15

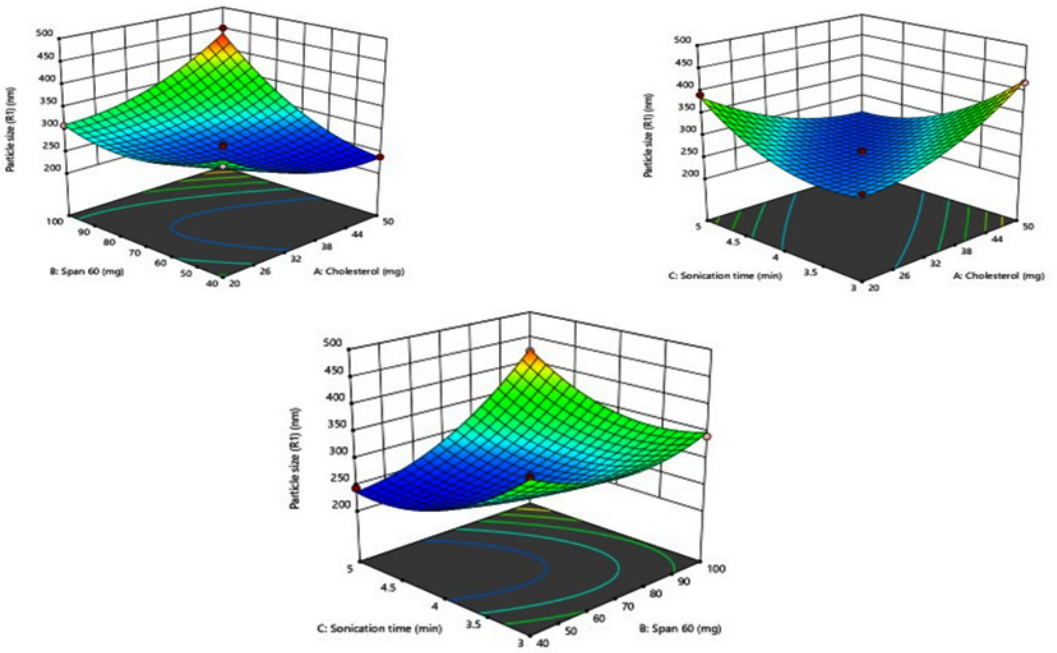

(A)

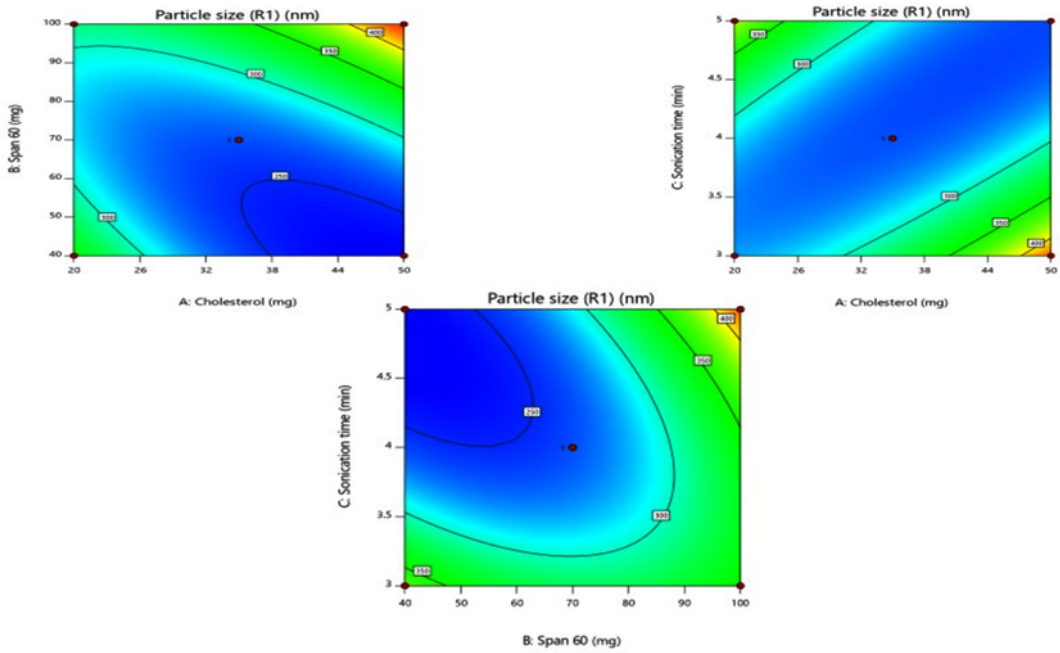

(B)

Fig. 1. A) Response surface plots and B) Contour plots illustrate the effect of cholesterol

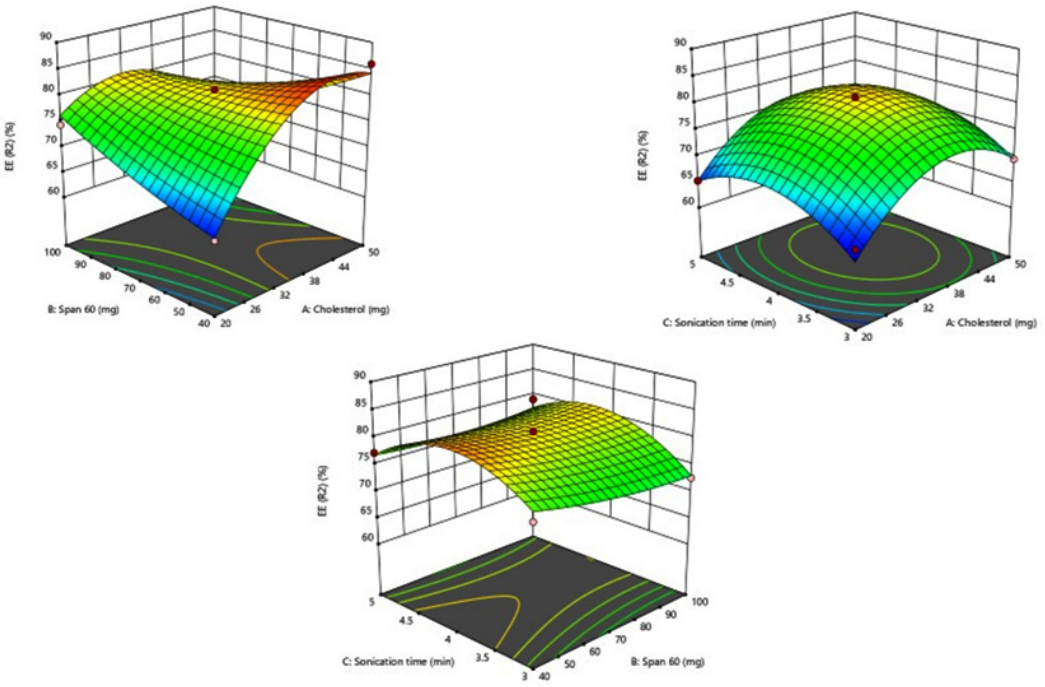

(X_1), span 60 (X_2), and sonication time (X_3) on vesicle size, respectively.

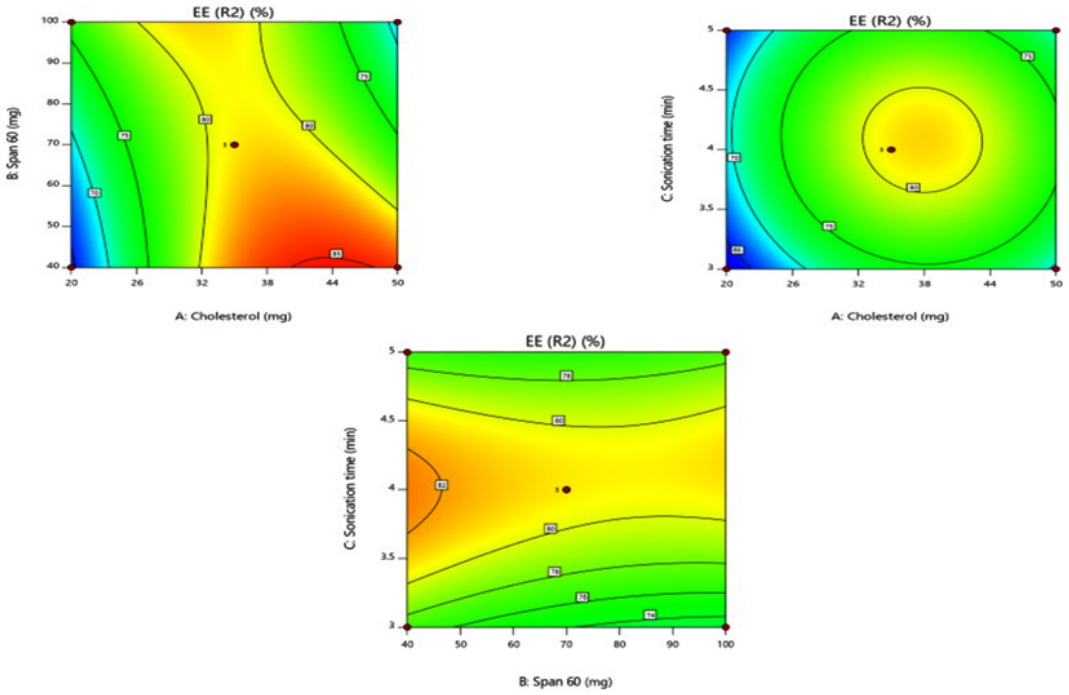

Fig. 2. A) Response surface plots and B) Contour plots illustrate the effect of cholesterol (X_1), span 60 (X_2), and sonication time (X_3) on % entrapment efficiency, respectively.

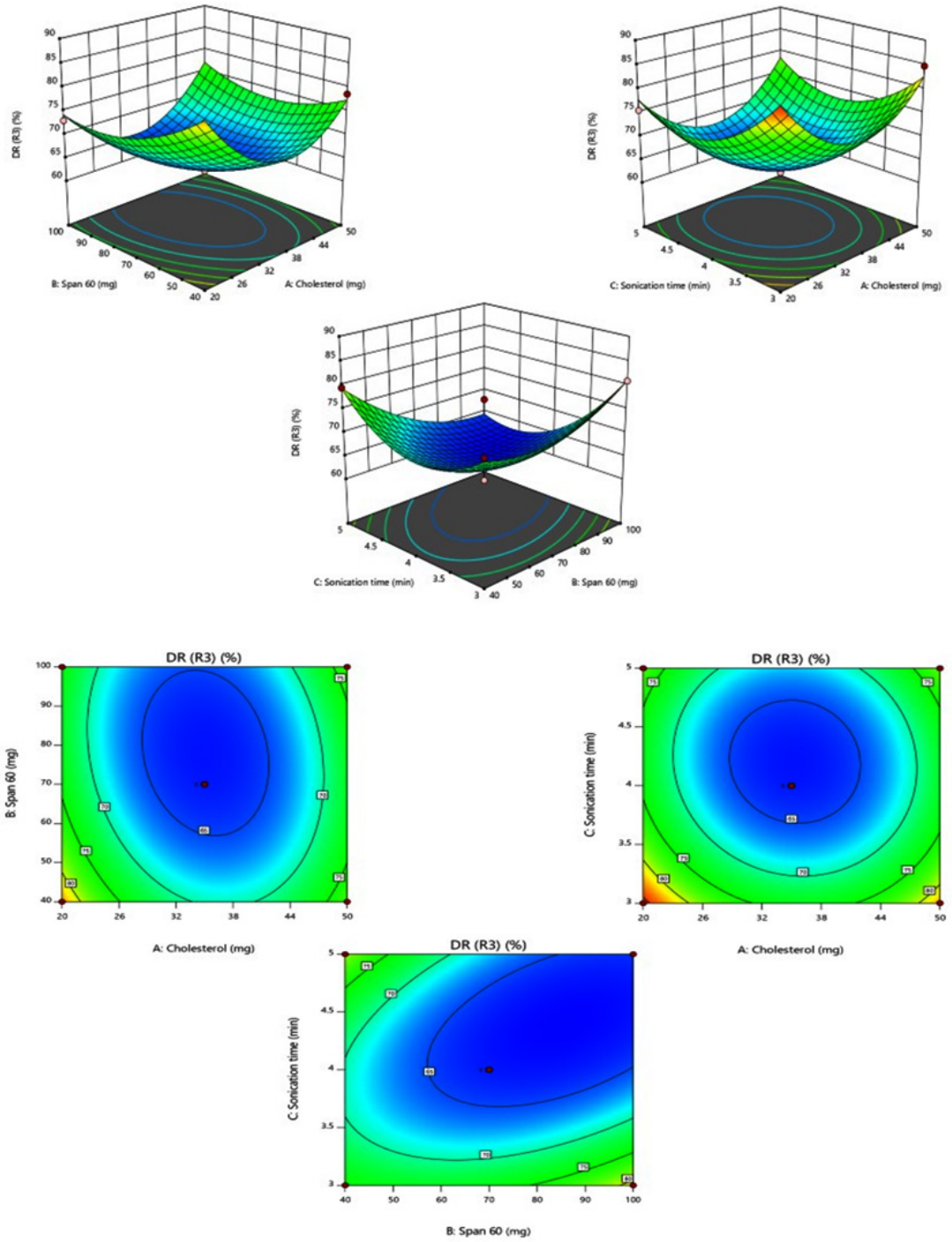

Fig. 3. A) Response surface plots and B) Contour plots illustrate the effect of cholesterol (X_1), span 60 (X_2), and sonication time (X3) on % drug release, respectively

temperature of 37 ± 0.5°C and a stirring speed of 100 rpm using a magnetic stirrer for 12 hours. To maintain a sink condition throughout the study, 2 mL samples were taken at specific intervals of 1, 2, 4, 6, 8, and 12 hours and immediately replaced with asimilar volume of PBS pH 7.4 freshly prepared. The quantity of drug released was measured from the collected samples using a UV spectrophotometer (Shimadzu 1800, Japan) (32). Drug release mechanisms have been studied using mathematical models, such as zero, first order, KorsmeyerPeppas and Higuchi. The results of *in vitro* drug release studies were verified to fit into different kinetic models, and correlation coefficient (R^2) values were calculated[31].

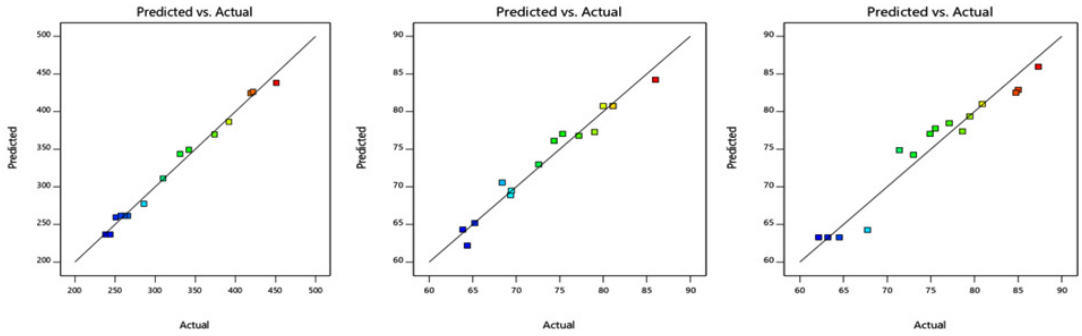

Fig. 4. Effect of the actual and predicted value of independent variables on vesicle size (R_1), EE (R_2), and DR (R_3)

Table 3. Summary for responses from regression analysis R_1 (Vesicle size), R_2 (EE), and R_3 (DR)

Statistical parameters	R_1	R_2	R_3
R^2	0.9904	0.9652	0.9415
Adjusted R^2	0.9732	0.9025	0.8362
Predicted R^2	0.8543	0.4603	0.1068
SD	11.96	2.15	3.25
C.V. %	3.70	2.92	4.33

Abbreviations: R^2 = Coefficient of correlation, SD = Standard deviation, C.V. % = Coefficient variation.

Storage stability studies as per ICH guidelines

According to ICH regulatory requirements, the final optimized batch was used for the stability studies. Two different storage conditions were utilized for niosomal formulations: refrigeration 4 ± 2°C temperature and room temperature 252°Cfor three months. The formulations were kept in glass vials with aluminum foil seals for the duration of the study. The stability test was evaluated after 1, 2, and 3 months based on physical changes, including color, size of vesicles, zeta potential, and %EE. [32,33]

Table 4. Analysis of variance (ANOVA) for Quadratic Model

Source	Sum of squares	df	Mean square	F-value	P-value	
Response 1: Vesicle size (R1)						
Model	73986.83	9	8220.76	57.47	0.0002	significant
Residual	715.17	5	143.03			
Cor Total	74702.00	14				
Response 2: EE (R2)						
Model	642.88	9	71.43	15.40	0.0039	significant
Residual	23.19	5	7.45			
Cor Total	666.06	14				
Response 3: DR (R3)						
Model	850.62	9	94.51	8.94	0.0133	significant
Residual	52.86	5	10.57			
Cor Total	903.48	14				

Statistical Analysis

Experiments were performed in triplicate to determine the mean and standard deviation. Utilising Design-Expert® Software (Version 11), statistical analysis, response surface methodology, and factorial optimization of the data were accomplished. Data evaluations were done using analysis of variance (ANOVA). When the applied model and correlation factor (R^2) were fitted, the value was deemed with a *p*-value less than significant.

RESULTS

The optimization data for the luteolin-loaded niosomes, the evaluation of the various statistical parameters and regression analysis utilized to analyze the different models, including linear, quadratic, 2FI, and cubic models, were observed, and the most appropriate quadratic model was found.The regression analysis response R^2 values of vesicle size (R1), EE (R2), and DR (R3) 0.9904, 0.9652, and 0.9415, respectively shown in

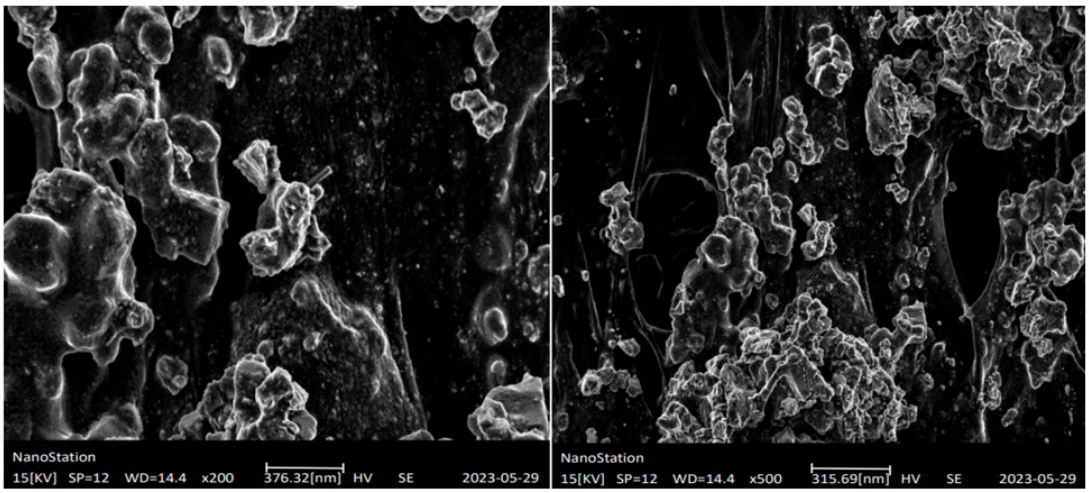

Fig. 5. SEM Image of optimized LUT loaded niosome (a) at 200x, (b) at 500x

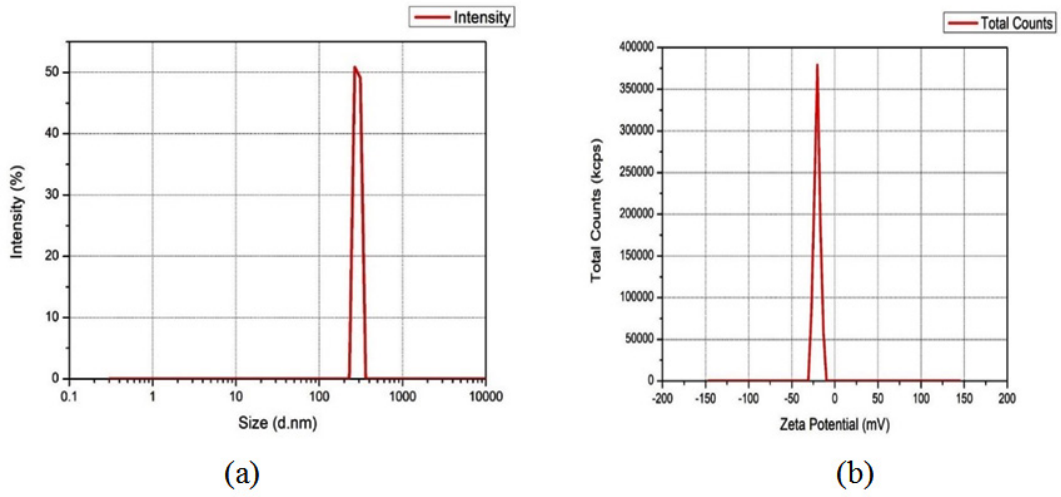

Fig. 6. (a) optimized batch of the Vesicle size (b)optimized batch of Zeta potential.

Table 3, and the ANOVA for the quadratic model was shown that R1, R2, and R3 were statistically significant *(p*< 0.005) from the ANOVA test depicted in Table 4. The R^2 and the ANOVA results confirmed the model was significant. Response surface and Contour plot Analysisas demonstrated in Figures 1, 2, and 3, respectively, 3D response surface plots, and contour plots are used to analyze the interaction between two factors and how the change in the amount of another factor would change the impact of one component. (Figure 4) illustrates the similarity between the actual and expected values graphically.[34]

Responses Evaluation

Vesicle morphology

The optimized LUT-loaded nucleus was found to have a spherical shape (Figure 5a and b) under a scanning electron microscope (SEM) at a nanosize scale of 376.32 nm at 200x magnification and 315.69 nm at higher magnification (500x).

Vesicle Size, PDI, and Zeta Potential

The vesicle sizes of all fifteen formulations were found to be 238–451 nm range. The formulation F14 showed the smallest vesicle size, and the formulation F3 showed a larger size. Resulting is the produced polynomial quadratic equation for the vesicle size:

$$\text{Vesicle size } (R_1) = +261.67 + 5.00\ X_1 + 42.25\ X_2 - 14.00\ X_3 + 58.50\ X_1X_2 - 68.50\ X_1X_3 + 52.50\ X_2X_3 + 31.17\ X_1^2 + 39.67\ X_2^2 + 44.17\ X_3^2 \quad ...(5)$$

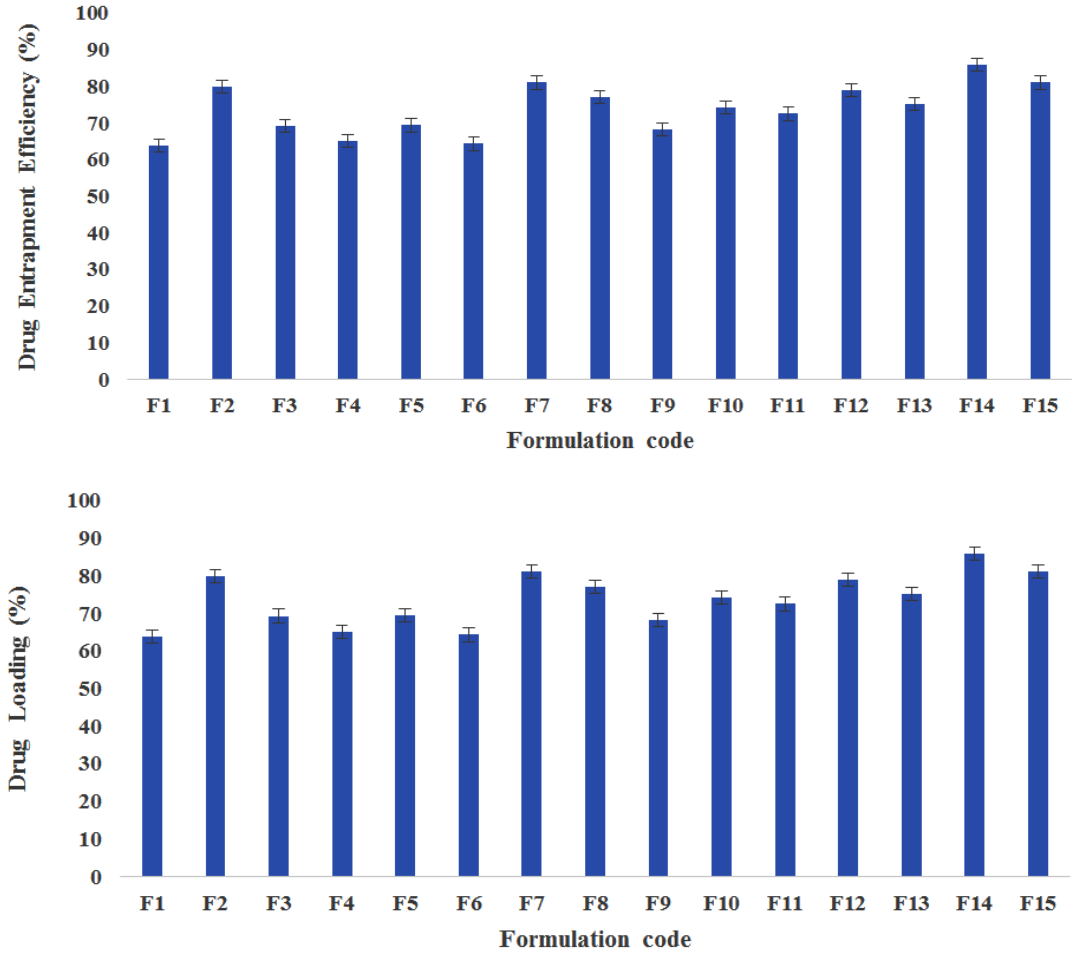

Fig. 7. Graph of (a)% Entrapment efficiency, (b) % Drug loading

The optimized formulation PDI value was found to be 0.34. PDI value 0-1 influence pharmacokinetic parameter of medicated NPs formulation on therapeutic performance[35].The optimized formulation's zeta potential was discovered to be -20.25 mV, less than -30 mV, indicating that the niosomal formulation is stable.[36,37] The graphs of vesicle size and ZP of the optimized LUT-loaded niosomes are shown in Figures 6 (a)and (b), respectively.

Table 5. Percentage drug EE and percentage DL of formulations

Formulation code	Entrapment efficiency (%)	Drug loading (%)
F1	63.86	53.22
F2	80	38.09
F3	69.35	23.12
F4	65.24	36.24
F5	69.44	28.93
F6	64.38	35.77
F7	81.12	38.62
F8	77.2	51.58
F9	68.39	28.13
F10	74.35	30.98
F11	72.58	26.88
F12	79	29.25
F13	75.33	35.87
F14	86	47.77
F15	81.12	38.62

Percentage Entrapment Efficiency and Drug Loading

The % EE and % DL valueof the LUT-loaded niosomes are presented in Table 5. The %EE depends on the type of encapsulated component, the vesicle material's characteristics, and the surfactants' qualities. It was observed that with the increasing lipid concentration, the % EE increased; the following is the produced polynomial quadratic equation for the EE:

$$EE\ (R_2) = +80.75 + 3.17\ X_1 - 0.8888\ X_2 + 1.01\ X_3 - 6.79\ X_1X_2 - 0.4775\ X_1X_3 + 1.14\ X_2X_3 - 8.26\ X_1^2 + 0.9042\ X_2^2 - 5.62\ X_3^2 \quad ...(6)$$

The % EE and % drug loading graphs are shown in Figure 7.

Fourier Transform Infra-Red

FTIR spectrum was conducted utilizing a Bruker FTIR instrument (Bruker FTIR Alpha 2, USA and USA and PerkinElmer L1600300 Spectrum TWO LiTa, Llantrisant, UK) was used to check the compatibility between LUT, span 60, cholesterol, and LUT loaded Niosome used.[38] The spectral peaks of Luteolin exhibited a wavenumber of 3205.70 cm^{-1}, ascribed to the OH group stretching vibration. The C=O stretching peaks were shown at 1666.15 cm^{-1}. The peaks of the aromatic ring, CH=CH stretching, C H, and ether

Table 6. Percentage In-vitro drug release profile of LUT loaded niosomes for different formulations at specific time 1,2,4,6,8 and 12 hours

Formulation Code	Time (hours) 1	2	4	6	8	12
F1	26.35	32.65	48.27	64.57	72.47	85.02
F2	18.34	24.3	32.9	40.02	48	64.52
F3	27.1	39.52	46.77	55.52	61.02	74.92
F4	13.45	20.25	37.52	49.65	58.47	75.52
F5	27.45	38.05	49.1	57.22	66.52	84.75
F6	21.27	36.22	49.72	62.57	74.37	87.32
F7	12.25	15.5	26.3	38	47.6	63.20
F8	30.92	35.54	45.22	54.82	62.8	79.47
F9	26.45	34.4	49.02	56.57	65.82	77.11
F10	28.77	37.35	43.77	56.1	61.37	73.02
F11	22.27	29.75	47.8	56.02	68.07	80.90
F12	10.32	15.6	24.6	37.82	46.97	67.75
F13	17.77	24.57	35.22	49.8	57.65	71.40
F14	28.82	31.04	42.53	53.55	60.39	78.62
F15	15.27	22	37.37	44.3	51.42	62.15

group are imputed at 633.73 cm^{-1}, 1306.02 cm^{-1}, 798.14 cm^{-1}, and 1124.24 $cm^{-1,}$ respectively, which was within the standard range. It is confirmed that the sample was luteolin (Figure 8 a). Span 60 showed spectra the OH group at wavenumber 3330.96 cm^{-1}, aromatic rings and alkanes at 1449.25 $cm^{-1,}$ and ether group at 1114.88 cm^{-1} (Figure 8b). Cholesterol OH group appears at wavenumber

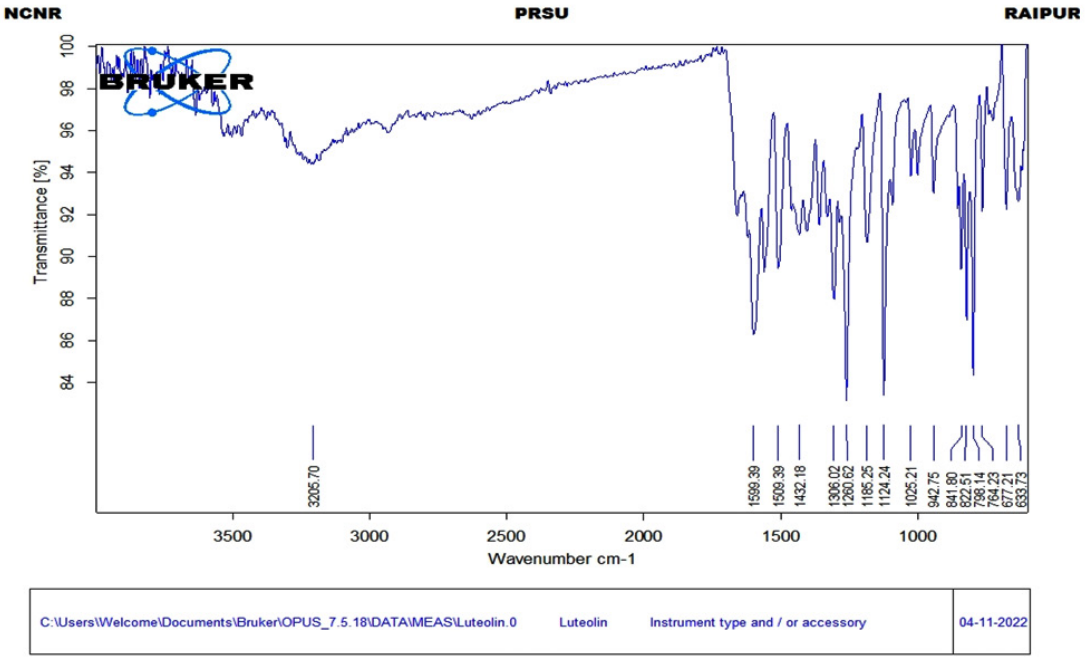

(a)

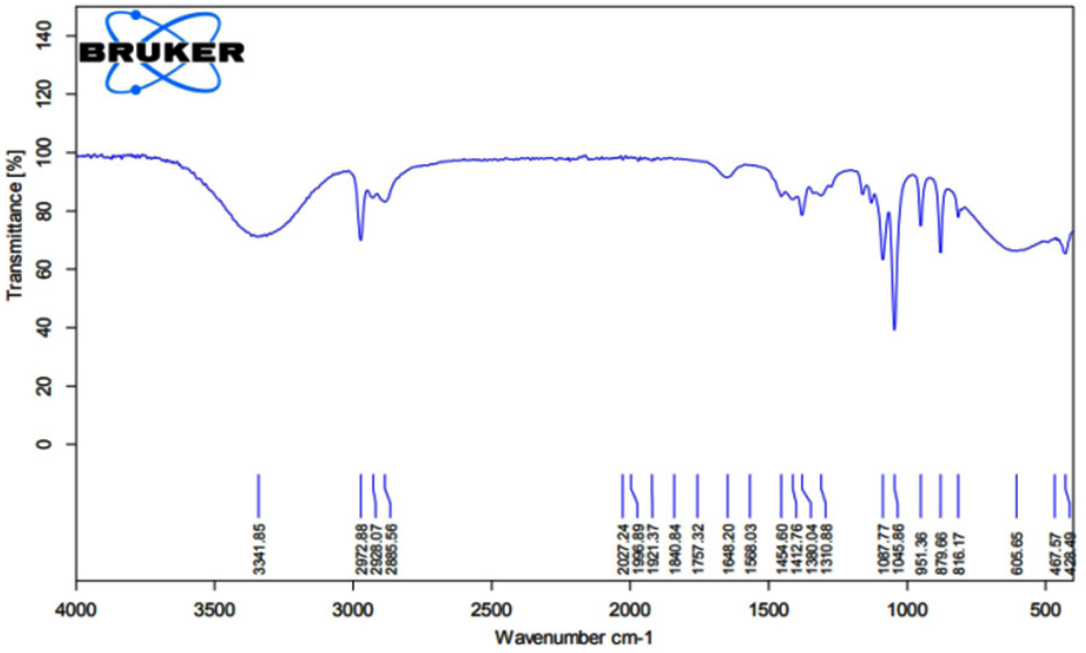

(b)

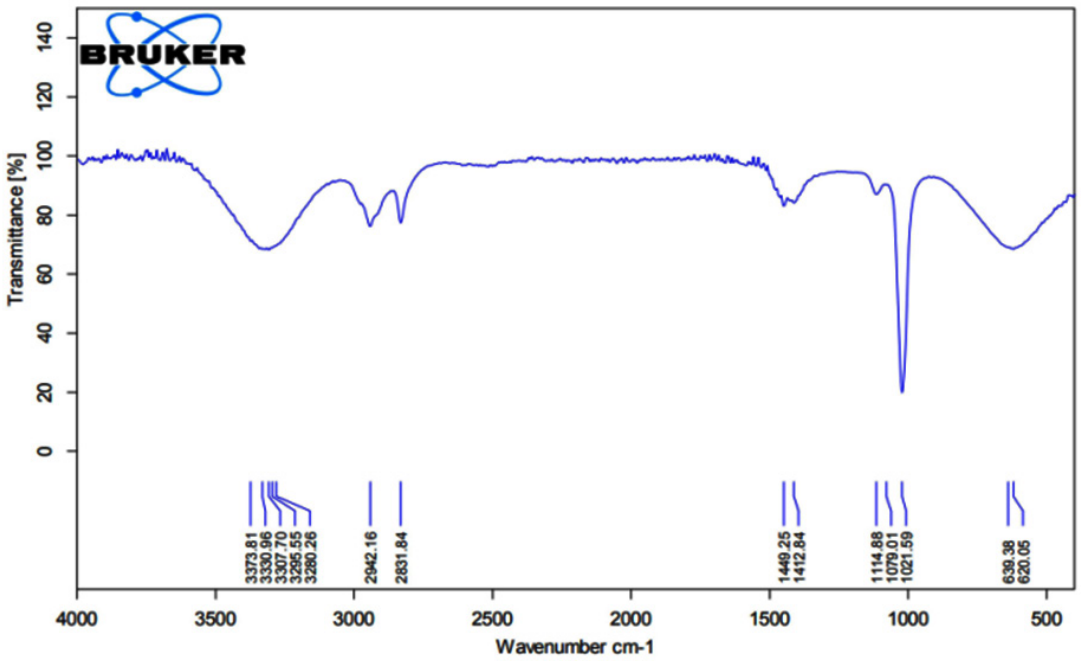

(c)

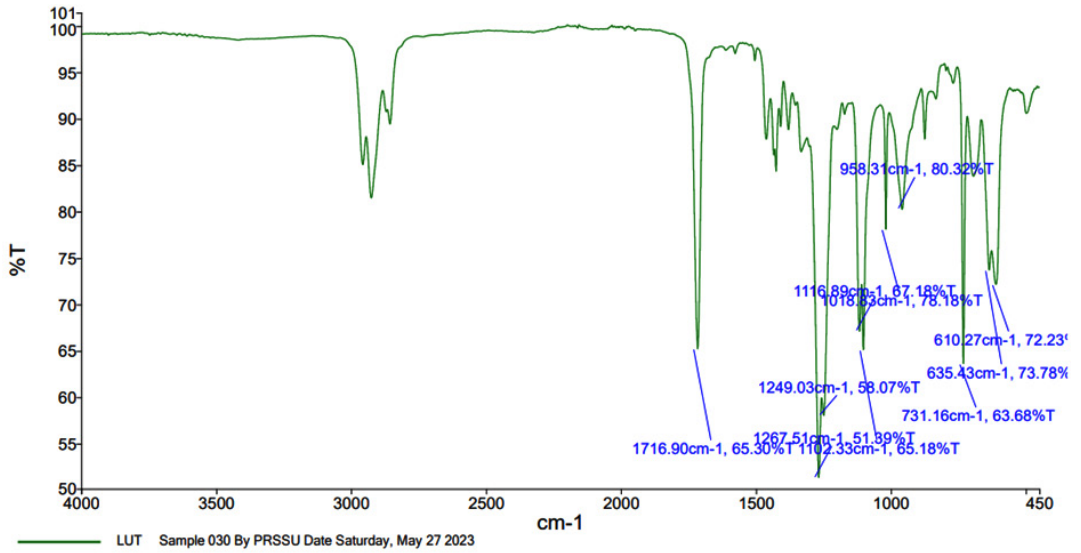

(d)

Fig. 8. (a). FTIR spectra of luteolin (b) Span 60 (c) cholesterol and (d) LUT loaded Niosome

3341.85 cm^{-1} and aromatic rings and alkanes at 1454.60 cm^{-1} (Figure 8c). LUT-loaded Niosomes FTIR spectra, a significant absorption peak at 3206 cm{ ¹ signifies the presence of an OH group. Within the spectral range of 1716-1509 cm{ ¹, peaks are observed, C=O stretching and C-H stretching vibrations. The region spanning 1432-1260 cm{ ¹ Moreover, at 1267-1249 cm{ ¹, a distinct peak is evidence of a carbonyl group integrated within the ring structure. These findings, derived from

the FTIR spectral analysis, offer scientifically significant insights into the compound's chemical composition and the specific functional groups it contains, shown in (Figure 8d).

***In-vitro* Drug Release**

The in *vitro* release of LUT from all Niosome preparations was investigated over 12 hours using the dialysis bag technique in PBS at pH 7.4. Pure LUT exhibited a rapid release ofaround 91% within the 3-hourinitial. This highlights the effectiveness of employing a dialysis bag to observe the release pattern of LUT from a prepared Niosome. Figure 9 shows the release profiles of LUT from different formulations (F1-F15) of Niosome. Notably, no immediate burstrelease of drug was observed in the Niosome formulations during the first 6 hours.The prepared LUT-loaded noisome and pure LUT for drug release is presented in Table 6. In the study's first 12 hours, the pure LUT had a poor drug release rate (23 percent) due to its poor solubility in water at the studied temperature. However, it is recommended to optimize the drug's release from the niosomes to better synchronize with the elevated solubility of LUT in the niosomes vesicle. The % DR of the optimised LUT-loaded niosomal suspension was 67.08% in 12 h (Table 7). The polynomial quadratic equation generated for the DR is given as follows:

$$\text{Drug release } (R_3) = +63.29 - 0.6850\ X_1 - 2.24\ X_2 - 3.07\ X_3 + 2.08\ X_1X_2 + 1.04\ X_1X_3 - 5.30\ X_2X_3 + 10.45\ X_1^2 + 4.16\ X_2^2 + 7.43\ X_3^2 \quad ...(7)$$

In the first four hours, about 40% of the drug was released; after that, the release was sustained

Table 7. *In-vitro* release of the optimized LUT loaded niosomes in PBS pH 7.4 at 37 ± 0.5°C

Time (hours)	Cumulative drug release (%)
1	11.24
2	16.82
4	26.41
6	38.11
8	46.39
12	67.08

Drug release kinetic model

The in *vitro* release kinetics of the optimized LUT-loaded phytosomes were examined, and their release patterns were analyzed using the Higuchi, Zero Order, Korsmeyer Peppas andFirst Ordermodels. The coefficient (R^2) values for the release of simple LUT-loaded niosomes F1 are 0.954, 0.997, 0.989, and 0.986 (n = 0.5). These results are summarized in Table 8, which includes data for F1-F15. The model with an R^2

Table 8. Release kinetic models of niosomal formulations

Formulation code	Release kinetic models							
	Zero-order		First order		Higuchi		Korsmeyer-Peppas	
	R^2	K_0	R^2	K_1	R^2	K_H	R^2	N
F1	0.954	5.519	0.997	-0.064	0.989	25.192	0.986	0.500
F2	0.997	4.101	0.985	-0.034	0.980	18.231	0.986	0.492
F3	0.961	4.034	0.988	-0.039	0.989	18.353	0.976	0.376
F4	0.975	5.679	0.996	-0.049	0.997	25.747	0.955	0.716
F5	0.986	4.975	0.969	-0.058	0.991	22.378	0.993	0.435
F6	0.951	5.841	0.995	-0.070	0.994	26.787	0.990	0.562
F7	0.993	4.790	0.994	-0.035	0.981	21.346	0.981	0.690
F8	0.998	4.426	0.979	-0.047	0.982	19.697	0.631	0.531
F9	0.959	4.564	0.997	-0.045	0.997	20.866	0.997	0.438
F10	0.970	3.955	0.994	-0.037	0.991	17.927	0.165	0.251
F11	0.962	5.365	0.996	-0.055	0.995	24.466	0.994	0.535
F12	0.998	5.254	0.977	-0.039	0.971	23.246	0.990	0.761
F13	0.977	4.962	0.997	-0.042	0.992	22.425	0.992	0.575
F14	0.995	4.630	0.975	-0.047	0.975	20.561	0.953	0.414
F15	0.948	4.226	0.986	-0.031	0.993	19.399	0.992	0.580

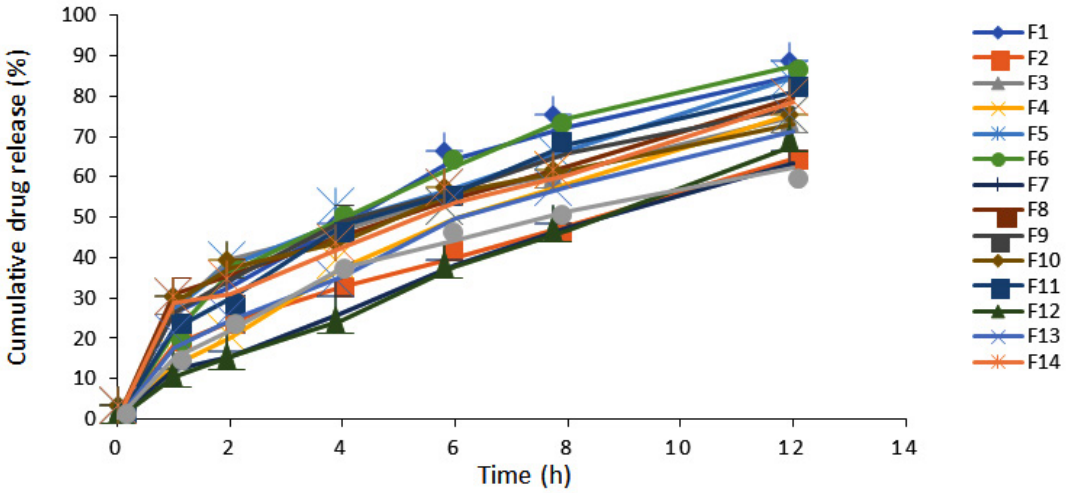

Fig. 9. *In-vitro* release profile of various LUT-loaded niosomes formulations (F1-F15) in PBS pH 7.4 at 37 ± 0.5°C.

Table 9. Comparison of the predicted and observed values of the LUT-loaded niosomes

Response variables	Optimized formula			Predicted value	Observed value	Bias %
	Cholesterol (mg)	Span 60 (mg)	Sonication time (min)			
Vesicle size (nm)				285.39	267.2	6.37
EE (%)	34.05	51.40	3.50	79.53	78.31	1.53
DR (%)				68.25	67.08	1.71

(EE) (79.53%), and DR (68.25%) in Table 9 closely matched the observed values

Table 10. Stability study of the optimized formulation 3 at 4 ±2

Parameter studies	Initial	After 3 months
Color	Off white	No change
Vesicle size (nm)	267.2	269.5
Zeta potential (mV)	-20.25	-19.51
Drug entrapment efficiency (%)	78.31	76.93

Table 11. Stability study of the optimized formulation 3 at 25 ± 2

Parameter studies	Initial	After 3 months
Color	Off white	No change
Vesicle size (nm)	267.2	274.7
Zeta potential (mV)	-20.25	-17.29
Drug entrapment efficiency (%)	78.31	72.59

value of one was measured the bestfit model for the formulations. According to the findings, all formulations with the first-order model were fairly linear. According to the KorsmeyerPeppas model, the value of *n* should be in the range of 0.45-0.89 of the standard value. The release exponent (n) value was found to be 0.25 to 0.71, indicatingFickian (class I) diffusion.

Point prediction

Optimized method using the point prediction, the formulation of the optimal niosomes was chosen. It provides a recipe for creating optimal niosomes. The ideal niosomes formulation was found to contain the following components: cholesterol (X_1) 34.05 mg, span 60 (X_2) 51.40 mg, and sonication time (X_3) 3.50 min. In the optimized formulation, the vesicle size measured 267.2 nm, with an entrapment efficiency of 78.31% and a drug release (DR) of 67.08% (Table 9). The predicted values for vesicle size (285.39 nm), entrapment efficiency (EE) (79.53%), and DR (68.25%) in Table 9 closely matched the observed values.

Storage stability studies as per ICH guidelines

The optimized formulation's stability was studied by storingit at 4 $\pm$ C (refrigeration) and 25C "room temperature" for 3 months. The color, vesicle size, zeta potential, and EE (%) were determined. The results indicated that the EE of the drug was more abundant in niosomal preparations stored at 4C (76.93% in Table 10) and 25C (72.59% in Table 11). An increase in temperature decreases the drug's EE capability due to the degradation of lipids. From the obtained data, it can be concluded that the optimum storage condition for niosomes was 4°C.

DISCUSSION

The optimization data for the luteolin-loaded niosomes was evaluated using various statistical parameters and regression analysis. The analysis considered multiple models, including linear, quadratic, 2FI, and cubic models, to determine the best fit. Among these, the quadratic model was identified as the most appropriate, demonstrating superior regression coefficients and statistical significance.The regression analysis revealed high R^2 values for the responses: vesicle size (R1 = 0.9904), encapsulation efficiency (EE, R2 = 0.9652), and drug release (DR, R3 = 0.9415), as detailed in Table 3. These values indicate a strong correlation between the independent and dependent variables, confirming the quadratic model's suitability. Adjusted R^2 values of 0.9732 for R1, 0.9025 for R2, and 0.8362 for R3 further support the model's reliability. However, predicted R^2 values were notably lower (0.8543, 0.4603, and 0.1068 for R1, R2, and R3, respectively), suggesting some limitations in the predictive accuracy for certain responses.The ANOVA results (Table 4) corroborated the statistical significance of the quadratic model for all responses, with p-values < 0.005. For vesicle size (R1), the model achieved an F-value of 57.47, and for EE (R2), the F-value was 15.40, indicating the strong influence of the independent variables on these responses.

This nanosized, spherical morphology is crucial for topical wound healing applications, as it allows for deeper penetration and enhanced cellular interaction within the wound bed. The surface area to volume ratio increased of these nanoparticles improves lutein's bioavailability, promoting its antioxidant and anti-inflammatory effects, essential for accelerating wound healing. The factors cholesterol and span 60 showed a positive effect, and the factor sonication time negatively impacted the vesicle size. When the lipid concentration increases, vesicle size also increases. The polydispersity index provides insight into the particle size distribution's uniformity. A value of <0.5 suggests a homogeneous and monodisperse formulation, indicating consistent particle sizes. Conversely, a polydispersity index >0.5 indicates less uniform size distribution or polydispersity within the formulation. Optimized preparations were successfully made, as predicted by the experimental design. PDI value 0-1 influences pharmacokinetic parameter of medicated NPs formulation on therapeutic performance [39].The lower value denotes a more uniform dispersion. Colloidal dispersion stability is often assessed through the measurement of zeta potential. Typically, a zeta potential outside the range of ±30 mV indicates the potential for particle aggregation can be mitigated through electrostatic repulsion. However, it is worth noting that various studies have demonstrated stable dispersions even with zeta potential values lower than this threshold, especially during storage. less than -30 mV, indicating that the niosomal formulation is stable[40]. The % EE and % DL values of the LUT-loaded niosomes. The %EE depends on the type of encapsulated component, the vesicle material's characteristics, and the surfactants' qualities. It was observed that with the increasing lipid concentration, the % EE increased. FTIR spectral analysis offers scientifically significant insights into the compound's chemical composition and

the specific functional groups it contains. There is no drug and excipient chemical interaction, as evidenced by the drug's LUT-loaded Niosomes FTIR spectra showed no change in their functional group regions.

The in *vitro* release of LUT from all Niosome preparations was investigated over 12 hours using the dialysis bag technique in a PBS at pH 7.4. Notably, no immediate brust release of drug was observed in the Niosome formulations during the first 6 hours.However, it is recommended to optimize the drug's release from the niosomes to better synchronize with the elevated solubility of LUT in the niosomes vesicle. According to the findings, all formulations with the first-order model were fairly linear. According to the Korsmeyer Peppas model, the value of *n* should be in the range of 0.45-0.89 of the standard value. The release exponent (n) value was found to be 0.25 to 0.71, indicating Fickian (class I) diffusion.Optimized method using the point prediction, the formulation of the optimal niosomes was chosen. The optimized formulation's stability was studied by storing it at 4 $\pm$ C (refrigeration) and 25C "room temperature" for 3 months. An increase in temperature decreases the drug's EE capability due to the degradation of lipids. From the obtained data, it can be concluded that the optimum storage condition for niosomes was 4°C.

CONCLUSIONS

This study focused on developing and thoroughly evaluating luteolin-loaded niosomes for their potential application in wound healing delivery. Using the Box-Behnken Design (BBD), we successfully optimized the formulation of luteolin-loaded niosomes using the Thin Film Hydration Method. Notably, the concentrations of surfactant and cholesterol significantly influenced both the encapsulation efficiency (EE) and release kinetics of luteolin, with higher lipid concentrations leading to increased EE. Our optimized niosome formulation exhibited favorable characteristics, including a vesicle size of 267.2 nm, a polydispersity index (PDI) of 0.34, a zeta potential of -20.25 mV, and an EE of 78.31%. Fourier-transform infrared (FTIR) spectra confirmed the presence of luteolin functional groups without any alterations in other excipients. Furthermore, our release studies conducted in phosphate-buffered saline (pH 7.4) demonstrated that the optimized luteolin-loaded niosomal suspension exhibited a drug release of 67.08% within 12 hours. The release kinetics followed a first-order reaction and exhibited Fickian diffusion, indicating prolonged drug release over 12 hours. This sustained release profile suggests the potential of our niosomes formulation to reduce dosing frequency, thereby enhancing therapeutic efficacy and patient adherence. Novelty in the study can be introduced by coating the niosomes to improve stability at 25ÚC.Further investigations could explore the in *vivo* efficacy and safety of the optimized luteolin-loaded niosomes in animal wound healing models. Additionally, efforts to fine-tune formulation parameters and explore alternative drug delivery methods could contribute to advancing the clinical translation of this promising approach. Ultimately, our study lays a solid foundation for future research endeavors to leverage the therapeutic potential of luteolin-loaded niosomes for enhanced wound healing outcomes.

ACKNOWLEDGMENTS

The authors thank the Director of the University Institute of Pharmacy, Pt. Ravishankar Shukla University, Raipur, Chhattisgarh, India, for the provision of essential infrastructural support.

Funding Sources

The author(s) received no financial support for the research, authorship, and/or publication of this article.

Conflict of interest

The authors do not have any conflict of interest.

Data Availability Statement

This statement does not apply to this article.

Ethics Statement

This research did not involve human participants, animal subjects, or any material that requires ethical approval.

Informed Consent Statement

This study did not involve human participants, and therefore, informed consent was not required.

Clinical Trial Registration

This research does not involve any clinical trials**.**

Permission to reproduce material from other sources

Not Applicable

Authors' Contribution

Devwati Puri: Conceptualization, Methodology, Writing – Original Draft; Harish Bhardwaj: Data Collection, Analysis, Writing – Review & Editing; Rajendra Kumar Jangde: Visualization, Supervision, Project Administration, Funding Acquisition.

REFERENCES

1. Krizanova O, Penesova A, Sokol J, Hokynkova A, Samadian A, Babula P. Signaling pathways in cutaneous wound healing. *Front Physiol*. 2022;13:1030851. Published 2022 Nov 25. doi:10.3389/fphys.2022.1030851
2. Nourian Dehkordi A, MirahmadiBabaheydari F, Chehelgerdi M, RaeisiDehkordi S. Skin tissue engineering: wound healing based on stem-cell-based therapeutic strategies. *Stem Cell Res Ther*. 2019;10(1):111. Published 2019 Mar 29. doi:10.1186/s13287-019-1212-2
3. Saoudi M, Badraoui R, Chira A, Saeed M, Bouali N, Elkahoui S, Alam JM, Kallel C, El Feki A. The Role of *Allium subhirsutum* L. in the Attenuation of Dermal Wounds by Modulating Oxidative Stress and Inflammation in *Wistar* Albino Rats [published correction appears in Molecules. 2022 Aug 22;27(16):5332. doi: 10.3390/molecules27165332]. *Molecules*. 2021;26(16):4875. Published 2021 Aug 12. doi:10.3390/molecules26164875
4. Bhardwaj H, Khute S, Sahu R, Jangde RK. Advanced Drug Delivery System for Management of Chronic Diabetes Wound Healing. *Curr Drug Targets*. 2023;24(16):1239-1259. doi:10.2174/0113894501260002231101080505
5. Borena BM, Martens A, Broeckx SY, Meyer E, Chiers K, Duchateau L, Spaas JH. Regenerative Skin Wound Healing in Mammals: State-of-the-Art on Growth Factor and Stem Cell Based Treatments. *Cell Physiol Biochem*. 2015;36(1):1-23. doi:10.1159/000374049
6. Fatima F, Aldawsari MF, Ahmed MM, Anwer MK, Naz M, Ansari MJ, Hamad AM, Zafar A, Jafar M. Green Synthesized Silver Nanoparticles Using Tridax Procumbens for Topical Application: Excision Wound Model and Histopathological Studies. *Pharmaceutics*. 2021;13(11):1754. Published 2021 Oct 21. doi:10.3390/pharmaceutics13111754
7. Anwer MK, Mohammad M, Iqbal M, Ansari MN, Ezzeldin E, Fatima F, Alshahrani SM, Aldawsari MF, Alalaiwe A, Alzahrani AA, Aldayel AM. Sustained release and enhanced oral bioavailability of rivaroxaban by PLGA nanoparticles with no food effect. *J Thromb Thrombolysis*. 2020;49(3):404-412. doi:10.1007/s11239-019-02022-5
8. Rodrigues M, Kosaric N, Bonham CA, Gurtner GC. Wound Healing: A Cellular Perspective. *Physiol Rev*. 2019;99(1):665-706. doi:10.1152/physrev.00067.2017
9. Aziz N, Kim MY, Cho JY. Anti-inflammatory effects of luteolin: A review of in vitro, in vivo, and in silico studies. *J Ethnopharmacol*. 2018;225:342-358. doi:10.1016/j.jep.2018.05.019
10. Gendrisch F, Esser PR, Schempp CM, Wölfle U. Luteolin as a modulator of skin aging and inflammation. *Biofactors*. 2021;47(2):170-180. doi:10.1002/biof.1699
11. Chen LY, Cheng HL, Kuan YH, Liang TJ, Chao YY, Lin HC. Therapeutic Potential of Luteolin on Impaired Wound Healing in Streptozotocin-Induced Rats. *Biomedicines*. 2021;9(7):761. Published 2021 Jun 30. doi:10.3390/biomedicines9070761
12. Sarawek S, Sasiporn D, Devendorf R, Butterweck V. Pharmacokinetics of luteolin and metabolites in rats. *Nat Prod Commun*. 2008;3(12):1934578X0800301218.
13. Taheri Y, Sharifi-Rad J, Antika G, Yýlmaz YB, Tumer TB, Abuhamdah S, Chandra S, Saklani S, Kýlýç CS, Sestito S, Daþtan SD. Paving Luteolin Therapeutic Potentialities and Agro-Food-Pharma Applications: Emphasis on *In Vivo* Pharmacological Effects and Bioavailability Traits. *Oxid Med Cell Longev*. 2021;2021:1987588. Published 2021 Sep 20. doi:10.1155/2021/1987588
14. Wu C, Xu Q, Chen X, Liu J. Delivery luteolin with folacin-modified nanoparticle for glioma therapy. *Int J Nanomedicine*. 2019;14:7515-7531. Published 2019 Sep 16. doi:10.2147/IJN.S214585
15. Wang L, Zhong C, Zu Y, Zhao X, Deng Y, Wu W, Sun X, Wang L, Wu M. Preparation and characterization of luteolin nanoparticles to enhance bioavailability and inhibit liver microsomal peroxidation in rats. *J Funct Foods*.2019;55:57-64.
16. Bhardwaj H, Jangde RK. Development and characterization of ferulic acid-loaded chitosan nanoparticle embedded- hydrogel for diabetic wound delivery. *Eur J Pharm Biopharm*. 2024;201:114371. doi:10.1016/j.ejpb.2024.114371
17. Gilani SJ, Bin-Jumah M, RizwanullahM, Imam

SS, Imtiyaz K, Alshehri S, Rizvi MM. Chitosan-coated luteolin nanostructured lipid carriers: Optimization, in vitro-ex vivo assessments, and cytotoxicity study in breast cancer cells. *Coatings.*2021;11:158.

18. Jangde RK, Khan T, Bhardwaj H. Development and characterization of nanostructured lipid carrier for topical delivery of naringenin. *Res J Pharm Tech.* 2023;16(5):2572-2576.
19. Wang Y, Wang Q, Feng W, Yuan Q, Qi X, Chen S, Yao P, Dai Q, Xia P, Zhang D, Sun F. Folic acid-modified ROS-responsive nanoparticles encapsulating luteolin for targeted breast cancer treatment. *Drug Deliv*. 2021;28(1):1695-1708. doi:10.1080/10717544.2021.1963351
20. Tawornchat P, Pattarakankul T, Palaga T, Intasanta V, Wanichwecharungruang S. Polymerized Luteolin Nanoparticles: Synthesis, Structure Elucidation, and Anti-Inflammatory Activity. *ACS Omega*. 2021;6(4):2846-2855. Published 2021 Jan 19. doi:10.1021/acsomega.0c05142
21. Kazmi I, Al-Abbasi FA, Nadeem MS, Altayb HN, Alshehri S, Imam SS. Formulation, Optimization and Evaluation of Luteolin-Loaded Topical Nanoparticulate Delivery System for the Skin Cancer. *Pharmaceutics*. 2021;13(11):1749. Published 2021 Oct 20. doi:10.3390/pharmaceutics13111749
22. Lalotra AS, Singh V, Khurana B, Agrawal S, Shrestha S, Arora D. A Comprehensive Review on Nanotechnology-Based Innovations in Topical Drug Delivery for the Treatment of Skin Cancer. *Curr Pharm Des*. 2020;26(44):5720-5731. doi:10.2174/1381612826666200819202821
23. Chen M, Shamim MA, Shahid A, Yeung S, Andresen BT, Wang J, Nekkanti V, Meyskens Jr FL, Kelly KM, Huang Y. Topical Delivery of Carvedilol Loaded Nano-Transfersomes for Skin Cancer Chemoprevention. *Pharmaceutics*. 2020;12(12):1151. Published 2020 Nov 27. doi:10.3390/pharmaceutics12121151
24. Griffith JW, Sokol CL, Luster AD. Chemokines and chemokine receptors: positioning cells for host defense and immunity. *Annu Rev Immunol*. 2014;32:659-702. doi:10.1146/annurev-immunol-032713-120145
25. Vadlamudi HC, Sevukarajan M. Niosomal drug delivery system: A review. *Indo Am J Pharm Res.* 2012;2(9).
26. Balakrishnan P, Shanmugam S, Lee WS, Lee WM, Kim JO, Oh DH, Kim DD, Kim JS, Yoo BK, Choi HG, Woo JS.Formulation and in vitro assessment of minoxidil niosomes for enhanced skin delivery. *Int J Pharm*. 2009;377(1-2):1-8. doi:10.1016/j.ijpharm.2009.04.020
27. Kazmi I, Al-Abbasi FA, Nadeem MS, Altayb HN, Alshehri S, Imam SS. Formulation, Optimization and Evaluation of Luteolin-Loaded Topical Nanoparticulate Delivery System for the Skin Cancer. *Pharmaceutics*. 2021;13(11):1749. Published 2021 Oct 20. doi:10.3390/pharmaceutics13111749
28. Danaei M, Dehghankhold M, Ataei S, Hasanzadeh F, Javanmard R, Dokhani A, Khorasani S, Mozafari MR. Impact of Particle Size and Polydispersity Index on the Clinical Applications of Lipidic Nanocarrier Systems. *Pharmaceutics*. 2018;10(2):57. Published 2018 May 18. doi:10.3390/pharmaceutics10020057
29. Bhardwaj H, Sahu RK, Jangde RK. Optimization and preparation of doxycycline-loaded chitosan nanoparticles using Box-Behnken design for better diabetic wound healing. *J Pharm Sci*. Published online December 2, 2024. doi:10.1016/j.xphs.2024.11.014
30. Abidin L, Mujeeb M, Imam SS, Aqil M, Khurana D. Enhanced transdermal delivery of luteolin via non-ionic surfactant-based vesicle: quality evaluation and anti-arthritic assessment. *Drug Deliv*. 2016;23(3):1079-1084. doi:10.3109/10717544.2014.945130
31. Laithy HM, Shoukry O, Mahran LG. Novel sugar esters proniosomes for transdermal delivery of vinpocetine: preclinical and clinical studies. *Eur J Pharm Biopharm*. 2011;77(1):43-55. doi:10.1016/j.ejpb.2010.10.011
32. Jangde R, Singh D. Preparation and optimization of quercetin-loaded liposomes for wound healing, using response surface methodology. *Artif Cells NanomedBiotechnol*. 2016;44(2):635-641. doi:10.3109/21691401.2014.975238
33. Byeon JC, Lee SE, Kim TH, Ahn JB, Kim DH, Choi JS, Park JS. Design of novel proliposome formulation for antioxidant peptide, glutathione with enhanced oral bioavailability and stability. *Drug Deliv*. 2019;26(1):216-225. doi:10.1080/10717544.2018.1551441
34. Alajami HN, Fouad EA, Ashour AE, Kumar A, Yassin AEB. Celecoxib-Loaded Solid Lipid Nanoparticles for Colon Delivery: Formulation Optimization and In Vitro Assessment of Anti-Cancer Activity. *Pharmaceutics*. 2022;14(1):131. Published 2022 Jan 5. doi:10.3390/pharmaceutics14010131
35. Shah HS, Gotecha A, Jetha D, Rajput A, Bariya A, Panchal S, Butani S. Gamma oryzanol niosomal gel for skin cancer: Formulation and optimization using quality by design (QbD) approach. *AAPS Open.*2021;7:1-5.
36. Aman RM, Zaghloul RA, Dahhan MS.

Formulation, optimization and characterization of allantoin-loaded chitosan nanoparticles to alleviate ethanol-induced gastric ulcer: in-vitro and in-vivo studies. *Sci Rep*. 2021;11(1):2216. Published 2021 Jan 26. doi:10.1038/s41598-021-81183-x

37. Epstein H, Gutman D, Sela E, Haber E, Elmalak O, Koroukhov N, Danenberg HD, Golomb G. Preparation of alendronate liposomes for enhanced stability and bioactivity: in vitro and in vivo characterization. *AAPS J*. 2008;10(4):505-515. doi:10.1208/s12248-008-9060-5
38. Shilakari Asthana G, Sharma PK, Asthana A. In Vitro and In Vivo Evaluation of Niosomal Formulation for Controlled Delivery of Clarithromycin. *Scientifica (Cairo)*. 2016;2016:6492953. doi:10.1155/2016/6492953
39. Zafar A, Alruwaili NK, Imam SS, Alotaibi NH, Alharbi KS, Afzal M, Ali R, Alshehri S, Alzarea SI, Elmowafy M, Alhakamy NA. Bioactive Apigenin loaded oral nano bilosomes: Formulation optimization to preclinical assessment. *Saudi Pharm J*. 2021;29(3):269-279. doi:10.1016/j.jsps.2021.02.003
40. Kaur M, Singh K, Jain SK. Luliconazole vesicular based gel formulations for its enhanced topical delivery. *J Liposome Res*. 2020;30(4):388-406. doi:10.1080/08982104.2019.1682602